Project Title

An improved model for operational specification of the electron density structure up to geosynchronous heights

Deliverable 002: Final Report

AOARD Contract No FA5209-09-P-0253

Authors

Anna Belehaki, Ioanna Tsagouri (National Observatory of Athens)
Ivan Kutiev, Pencho Marinov (Bulgarian Academy of Sciences)

July 2010

Report Documentation Page

Form Approved
OMB No. 0704-0188

1. REPORT DATE	2. REPORT TYPE	3. DATES COVERED
03 AUG 2010	**Final**	**03-08-2009 to 02-08-2010**

4. TITLE AND SUBTITLE
An improved model for operational specification of the electron density structure up to geosynchronous

5a. CONTRACT NUMBER
FA520909P0253

5b. GRANT NUMBER

5c. PROGRAM ELEMENT NUMBER

6. AUTHOR(S)
Anna Belehaki

5d. PROJECT NUMBER

5e. TASK NUMBER

5f. WORK UNIT NUMBER

7. PERFORMING ORGANIZATION NAME(S) AND ADDRESS(ES)
National Observatory of Athens,Metaxa and Vas. Pavlou,Palaia Penteli, Greece,GE,15236

8. PERFORMING ORGANIZATION REPORT NUMBER
N/A

9. SPONSORING/MONITORING AGENCY NAME(S) AND ADDRESS(ES)
Asian Office of Aerospace Research & Development, (AOARD), Unit 45002, APO, AP, 96338-5002

10. SPONSOR/MONITOR'S ACRONYM(S)
AOARD

11. SPONSOR/MONITOR'S REPORT NUMBER(S)
AOARD-094159

12. DISTRIBUTION/AVAILABILITY STATEMENT
Approved for public release; distribution unlimited

13. SUPPLEMENTARY NOTES

14. ABSTRACT
This report presents the final results of the project ?An improved model for operational specification of the electron density structure up to geosynchronous heights,? with the following main objectives a) To upgrade the Topside Sounder Model Profiler (TSMP) and the TSMP-assisted Digisonde (TaD) model b) To validate the results using ISR and topside electron density profiles, GNSS TEC and partial TEC parameters c) To specify added-value products based on the TaD functional capabilities d) To implement the TaD model on-line ingesting auto-scaled ionospheric parameters from Athens Digisonde e) To develop a prototype web service demonstrating the functionality of TaD to operate online using as input auto-scaled ionospheric parameters; and f) To demonstrate some of the indicative value-added products derived from the TaD outputs.

15. SUBJECT TERMS
Atmospheric Science, Atmospheric Electricity

16. SECURITY CLASSIFICATION OF:			17. LIMITATION OF ABSTRACT	18. NUMBER OF PAGES	19a. NAME OF RESPONSIBLE PERSON
a. REPORT	b. ABSTRACT	c. THIS PAGE			
unclassified	**unclassified**	**unclassified**	**Same as Report (SAR)**	**44**	

Table of Contents

List of Figures

Abstract

This report presents the final results of the project "An improved model for operational specification of the electron density structure up to geosynchronous heights" (FA5209-09-P-0253) with the following main objectives:

a) To upgrade the TaD model
b) To validate the results using ISR and topside electron density profiles, GNSS TEC and partial TEC parameters
c) To specify added-value products based on the TaD functional capabilities
d) To implement the TaD model on-line ingesting autoscaled ionospheric parameters from Athens Digisonde
e) To develop a prototype web service demonstrating the functionality of TaD to operate on-line using as input autoscaled ionospheric parameters and
f) To demonstrate some of the indicative value-added products derived from the TaD outputs.

Introduction

Description of the problem

The safety and security of space operations requires that spacecraft operators know and understand the environment around their spacecraft. A measure of the ionospheric element of that environment is given by the precise values of the total electron content (TEC) between the spacecraft and some location on the surface of the Earth (partial TEC) – and in some cases between two spacecrafts. The partial TEC value differs from those derived from ground-based GNSS receivers. The latter values represent the TEC of the whole ionosphere-plasmasphere system, i.e. height-integrated from the surface to the GNSS satellites around 20000 km altitude. For many space activities we must partition GNSS TEC above and below the spacecraft in order to derive the TEC applicable to a particular activity.

As direct observations of electron density are sparse, precise estimation of the partial TEC requires better modelling of the topside ionosphere, i.e. the region above peak electron density and that gradually merges into the plasmasphere at altitudes above the O^+- H^+ transition height. The topside is the region that contains most of the plasma that contributes to the TEC values that we seek to estimate; typically only 25% is below the F2 peak while typically < 10% comes from the plasmasphere. Furthermore, the topside is the region in which most LEO spacecraft operate, so accurate estimates of the TEC relevant to a particular spacecraft activity require us to partition the TEC within the topside. Thus modelling the topside electron density is central to our key objective.

Along this direction, Kutiev and Marinov (2007) and Kutiev et al. (2006 and 2007) developed an empirical model of the O^+- H^+ transition height (h_T), the topside electron density scale height (H_T) and their ratio $Rt=H_T/h_T$, named Topside Sounder Model (TSM) based on the Alouette/ISIS database. To further approach the problem of developing a topside/plasmaspheric electron density reconstruction model with increased accuracy, Kutiev et al. (2009a) offered analytical formulas for obtaining the shape of the vertical plasma

distribution in the topside ionosphere and plasmasphere based on TSM parameters. This profiler was named Topside Sounder Model Profiler (TSMP), which models separately the O^+ and H^+ density profiles. To obtain the density distribution, it needs specification of the F layer maximum density (NmF2), its height (hmF2) and its scale height (Hm) at its lower boundary. Recently, Kutiev et al., (2009b) applied TSMP to Digisonde measurements to reconstruct the electron density profile from the F layer peak to GNSS orbits (TaD model). A new expression of H^+ scale height in the plasmasphere was extracted from ISIS-1 topside sounder data, as a function of geomagnetic latitude. The verification of the TaD model has been attempted by Belehaki et al. (2009a), comparing the integral of TaD profiles with total electron content (TEC) measured by the CHAMP satellite (from 400 km up to GPS orbits) and by ground-based GPS receivers. The fitting between the measured GPS-TEC and the TaD-TEC depends a lot from the geographic location of the test site while the comparison with CHAMP TEC data showed some deviations that could be also attributed to the background models applied to reconstruct the CHAMP electron density profiles. Overall, the results from the first verification analysis revealed the need for further improvements, which is the main objective of this project.

Summary of the main results

In the frames of this project the Topside Sounders Model assisted by Digisonde (TaD) is further improved (**Section 1**) according to the following methodology: a) Improvement of the TaD scaling technique based on the calculation of O^+, H^+, and He^+ density distributions in transition region between topside F region and plasmasphere, extracted from the analysis of the electron density profiles from ISIS-1. This yield a more reliable determination of important scale height parameters (O^+, H^+, and He^+) and transition height; b) Improvements of the TSMP formulation to achieve optimization of the TaD algorithm. The main model expressions were revised to include He^+ distribution as a function of geomagnetic latitude and local time.

A systematic validation of the new profiler is presented in **Section 2** using Topside and ISR Electron Density Profiles (EDP), TEC and partial TEC parameters. The results show reduction of the model error 2.25 times in comparison to the previous version of the TaD model. Validation of the model results based on comparison with ISIS1 EDP shows clearly the model's ability to reproduce with impressive accuracy the ISIS1 EDP (98.8%). Systematical comparison between the O^+ distribution of TaD and measured EDP from the Malvern ISR gave a mean RMSE of 12% while this error increased slightly when compared between the total electron density and the observed values. A discussion related to these results is given in the last part of this Section.

Based on TaD capabilities and on users' requests we have been able to specify and develop a set of value added products, available through this prototype web service, while additional products have been specified (**Section 3**) for future implementation in the DIAS system.

The results from the optimized TaD algorithm are given in **Section 4**, and are available on-line through the web address http://www.iono.noa.gr/ElectronDensity/EDProfile.php. For this on-line implementation, autoscaled data from Athens Digisonde are ingested in the algorithm, to simulate real-time operation conditions. A technical failure in Athens Digisonde prevented

us to run in real-time this prototype web service. The Athens Digisonde is currently out of operation due to technical failure caused by a severe thunderstorm with lightning activity that hit Penteli area on Saturday 3 July 2010. The functionality of the prototype in real-time conditions will be resumed as soon as the Athens Digisonde becomes fully operational again. Currently this prototype web service provides data and value added products for four years period: 22 July 2006 to 2 July 2010.

In our attempt to validate the TaD results and demonstrate the functionality of the algorithms in real-time, we have specified a number of issues that should be considered in the future, especially when this model is going to be integrated to the DIAS system, and develop products based on real-time data from a number of ionospheric stations, such as maps of TEC. These issues among others are discussed in **Section 5**: Future steps.

1. Development of the advanced model for the electron density reconstruction up to geosynchronous height

1.1 Background models

The development of the advanced model for the electron density reconstruction up to geosynchronous height accomplished within this project continued a series of successive approximations to the open issue of the reconstruction of the electron density profile up to plasmaspheric heights. The improved technique is based on: i) the Topside Sounders Model (TSM), ii) the Topside Sounder Model Profiler (TSMP) and iii) the TSMP-assisted Digisonde (TaD) profile.

The Topside Sounders Model (TSM) reproduces the O^+- H^+ (upper) transition height (h_T) and the topside electron density scale height (H_T), based on 172,622 measured Ne profiles by topside sounders on Alouette-1a, -1b, -1c and -2 and ISIS-1 and –2 satellites (Bilitza, 2001). The H_T and h_T models are represented by 5-dimensional polynomials expressing both quantities as functions of month of the year, geomagnetic latitude, local time, solar flux F_{107}, and the geomagnetic index Kp. Later, Kutiev and Marinov (2007) developed a model of the ratio $Rt=H_T/h_T$, based on ratios of individual profiles and combined the three models into a single model named Topside Sounder Model (TSM). The key element in the modeling is the assumption that the lowest gradient on the topside Ne profile represents the altitude gradient of the O^+ density profile. Assuming exponential distribution of O^+ density, the transition height h_T is found at the height, where the upward extrapolated O^+ density becomes one half of the measured Ne density. The O^+ gradient, inferred from the Ne profile is converted into scale height, e.g. the distance in km at which the O^+ density changes *e* (Euler's number) times. Therefore, both H_T and h_T have the same dimension. TSM provides the topside F region scale height H_T and transition height h_T between O^+ and H^+ dominant regions, based on measured data only. As these parameters are intrinsic to plasma distribution in ionosphere and plasmasphere, they can be used in any model dealing with the plasma density structure. It has to be noted, that H_T is a vertical scale height and differ from the theoretical plasma scale height defined along magnetic field lines (see Belehaki et al., 2006).
Validation tests of TSM performance include the comparison with two of the most popular ionospheric profile reconstruction techniques, the Parametirized Ionospheric Model – PIM (Daniell et al., 1995) and the NeQuick model (Hochegger et al., 2000; Radicella and Leitinger, 2001). The results provide usefull input of the model's performance regarding the season and the solar activity level (Stankov et al., 2007).

Topside Sounder Model Profiler (TSMP): Most recently, Kutiev et al. (2006) offered a method for obtaining the shape of the vertical plasma distribution in topside ionosphere and plasmasphere by introducing H_T and h_T parameters into three well known formulas describing the vertical plasma distribution: α-Chapman, Sech-squared, and Exponential (see Stankov et al., 2003). The analytical formulas containing H_T and h_T were named as Topside Sounder

Model Profiler (TSMP). TSMP provides the shape of the vertical plasma distribution; the density distribution is obtained once the F layer density (NmF2) and height hmF2 at its lower boundary is specified.

TSMP provides the shape of the topside N(h) profile as the sum of the O^+ and H^+ profiles from hmF2 up to GPS heights. The O^+ profile takes H_T as its own scale height (H_{O+}= H_T), at transition height h_T both densities equalize, and above H^+ scale height (H_H^+) is taken as 16 times O^+ scale height. Later, Kutiev et al. (2009b; 2009c) found that the H_H^+/H_{O+} (or Hp/H_T) ratio is not constant with a value of 16, but depends on latitude and on average ranges between 12 and 4. The present formulation of TSMP has the form:

$$Ne = N_{O^+}(h) + N_{O^+}(h_T)\exp\left(-\frac{|h-h_T|}{Hp}\right) \quad (1)$$

where:

$$N_{O+}(h) = N_m \exp\left\{\frac{1}{2}\left[1-\frac{h-h_m}{H_{O^+}}-\exp\left(-\frac{h-h_m}{H_{O^+}}\right)\right]\right\}$$

Here Ne is the electron density assumed to be equal to the sum of O^+ and H^+ densities (Ne = N_{O+}+ N_{H+}) in all altitudes. N_{O+} is described by α-Chapman function, with a scale height H_{O+} being one half of H_T, while N_{H+} is pure exponential function with a scale height H_H^+ denoted as Hp. Below h_T, N_H^+ is forced to decrease by taking absolute difference |h- h_T | in order to comply with the real distribution. Therefore, the maximum of N_{H+} distribution is fixed at transition height, although in reality it lies slightly above. At transition height, N_{H+} = N_{O+}(h_T) and scale the hydrogen ion distribution in plasmasphere. To calculate the topside density profile, TSMP needs values of NmF2 and hmF2 at the lower boundary (denoted as *Nm* and *hm*).

TSMP-assisted Digisonde (TaD) profile: As mentioned above, TSM provides also the ratio Rt=H_T/h_T, which is not directly used in TSMP. The model ratio Rt, which actually over-determine the Ne profile, possess an important property: it can be used as a link between TSM parameters and another measured topside quantities. This property is used by Kutiev et al. (2009a) to link TSMP to Digisonde topside profiling technique. The new hybrid profiler, named TSMP-assisted Digisonde (TaD) profiler, uses ionogram-derived scale height at hmF2 (denoted as Hm), corrected in a way to comply with TSM-produced H_T. This correction factor depends on the location, but in conducted analysis an average value of 1.25 was taken. Therefore the corrected scale height is calculated as Hd = 1.25Hm. Further, TaD uses the model ratio Rt to obtain its actual transition height h_{TD} multiplying Hd by Rt. It was found that the plasmasphere scale height H_{H+} (now denoted as H_P) is not equal to 16 times H_T, as assumed from theoretical considerations, but it is latitude dependent, ranging in average from

about 12 at equator to 5 at 80° geomagnetic latitude. An empirical relation was introduced, defining $H_P = (9.\cos2(glat)+4)Hd$, where *glat* was geomagnetic latitude.
In TaD approach, the lower boundary values and the scale height are provided by Digisonde measurements. In other words, TaD feeds TSMP with Digisonde data. This combination makes TaD profiling connected with measurements and offers variety of applications, especially the reconstruction of actual Ne profiles over each Digisonde location. This property of TaD can be directly implemented in any regional digisonde network such as the European DIAS system to provide 3-D distribution (latitude, longitude, altitude) of electron density in real time

Belehaki et al. (2009a) conducted an extensive work on **verification of TaD** profiling technique by comparing the integral of TaD profiles with total electron content (TEC) measured by CHAMP satellite (from 400 km up to GPS orbits) and ground-based GPS receivers at locations of Athens and Juliusruh. Comparison of TaD with CHAMP-derived TEC showed standard deviation of 4.6 and 3.4 TECU and correlation coefficient of 0.86 and 0.81 for Athens and Juliusruh respectively. Comparison with ground-based TEC yielded a standard deviation of 5.3 and 2.9 TECU and correlation coefficient of 0.92 and 0.95 for corresponding locations.

1.2. Development of the improved TaD model

1.2.1. Improvement of the scaling technique

In the Interim report (Belehaki et al., 2009b), we stressed attention on the problem of how well TaD profiler describes the transition region between the topside F region and plasmasphere. We found that a certain number of Ne profiles measured by ISIS-1 topside sounder require additional amount of light ions to that of H^+ in order to equalize O^+ density at transition height h_T. We assumed that these Ne profiles indicated the presence of He^+ ions (Heelis et al., 1990; Su et al., 2005) and showed the latitude and local time distribution of the He^+ density, shown in **Figure 1**. We also included the helium ion density in the TSMP formula describing the electron density as a function of altitude by introducing a new parameter *g* being the ratio of H^+ and O^+ densities, $g = n(H^+)/n(O^+)$. TSMP formula is now given in the form:

$$Ne = N_{O^+}(h) + gN_{O^+}(h_T)\exp\left(-\frac{|h-h_T|}{Hp}\right) + (1-g)N_{O^+}(h_T)\exp\left(-\frac{|h-h_T|}{4H_T}\right) \qquad (2)$$

In the absence of He^+, $g = 1$ and the third term is equal to zero. The lower is *g*, the more He^+ ions are present. Obviously, *g* should be a function of geomagnetic latitude, local time and probably to the season. It is reasonable to assume that He^+ has its maximum again at the transition height, h_T, and exhibits a pure exponential distribution above, with a scale height

equal to 4 times that of H_T. However at higher latitudes, for the plasmaspheric scale height Hp, which theoretically should be 16 times that of H_T, this factor drops significantly due to the shape of plasmasphere. Having in mind this fact, here we try to infer the factor $s = H_{He+}/H_T$ from the data. We further denote He^+ scale height (H_{He+}) as H_E. So, formula (2) is now modified as in last exponent instead of $4H_T$ we place sH_T and the new TSMP formula is given by the following equation:

$$Ne = N_{O^+}(h) + gN_{O^+}(h_T)\exp\left(-\frac{|h-h_T|}{Hp}\right) + (1-g)N_{O^+}(h_T)\exp\left(-\frac{|h-h_T|}{sH_T}\right) \quad (3)$$

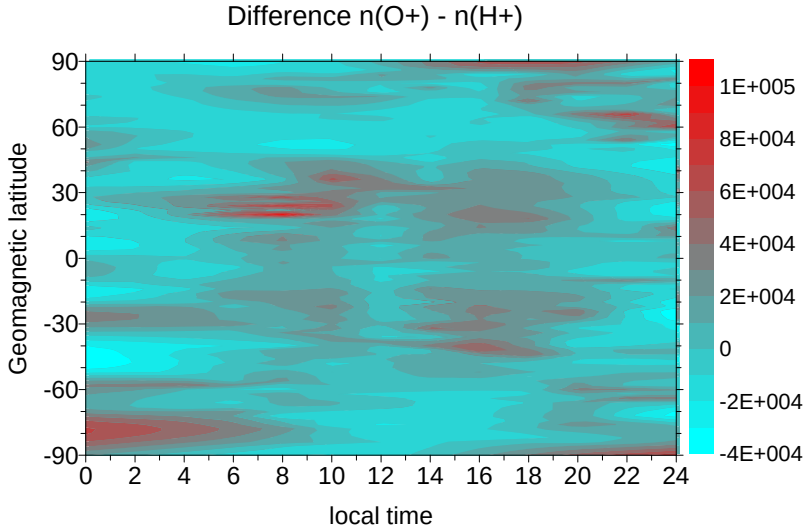

Figure 1: The geomagnetic latitude/local time contour map of the difference of O^+ and H^+ densities at transition height.

By definition He^+ density strongly depends on O^+ and H^+ densities at transition height, which in their turn strongly depend on scale heights H_T and Hp, determined from lowest and highest altitude gradients of the measured Ne profiles. Increasing the accuracy of fitting the measured Ne profiles in transition region comes up through the increase of the accuracy of He^+ determination at h_T. **To increase the accuracy of Hp and H_T, we developed a sophisticated algorithm, based on optimization of H_T, Hp, and *s* towards best fitting with measured Ne profile.** Formula (3) is run multiple times by using a set of H_T, Hp, and *s* and the model profile at each run is compared with measured Ne profile by calculating the root mean square (RMS) error. A series of values is assigned for each of these variables and Ne is calculated from formula (3), executing three nested cycles: the outer for H_T, middle for Hp and internal for *s*. Each run takes one of the H_T values, calculates the corresponding h_T, takes one of the Hp values, calculates the ratio *g* at h_T, takes one of the *s* values, and then calculates based on formula (3) the whole profile in the altitude range corresponding to the measured profile. The RMS error is stores and the next cycle is performed. We have set 40 values around the minimum H_T, 40 values around maximum Hp, and 120 values of *s* around 4. The whole optimization of a given profile contains 40 x 40 x 120 = 192,000 runs. So, we select the set of

the three variables that has the smallest RMS error. In this way we perform optimization to 14,775 measured ISIS-1 profiles. **Figure 2** shows, as a sample, the profile measured on day 97 of year 1969, 17:03 UT around equator (lat = 12˚S, long=12.5˚E). Logarithm of ion density profiles obtained without optimization (denoted as "old") and those with optimization (denoted by "new"), are color coded, along with the measured Ne profile presented with the black line. The "old" profiles are presented by dashed lines, while the "new" profiles are given by solid lines. The total ion density presented the sum of the "new" profiles is given by the orange line. In this sample, optimization increases slightly the values of H_T and h_T and reduces Hp. Optimization invokes its largest effect on He^+ density, which is substantially reduced. However, He^+ density profile below transition height h_T depends strongly on H^+ density shape, which as we have demonstrated, could not represent the real situation. As we are interested in reconstructing the electron density profile, which below h_T is mainly defined by O^+, the shape of H^+ is not important. The same is true for the He^+ profile below h_T. In this study we are mainly interested in He^+ density around its maximum fixed at h_T. The standard deviation of the optimized model from measured profiles, denoted as RMS, is 0.051, while that without optimization is 0.112 units of logarithm density. Here optimization has reduced RMS error more than twice.

We found that the He^+ scale height cannot be reliably obtained. Indeed, the RMS error is formed by comparing formula (3) with the whole measured profile. He^+ density in some cases is comparable with electron density within the transition region, but it is always much smaller outside that region and its net contribution to the RMS error is negligible. When calculating procedure executes formula (3) for variables in the nested cycles, RMS errors are practically determined by the pairs of H_T and Hp values, with no significance of values of *s*. Thus *s* value could not be optimized. Statistically for the whole database, s values are spread almost uniformly in the defined range. Taking into account this fact, we further take $s = 4$.

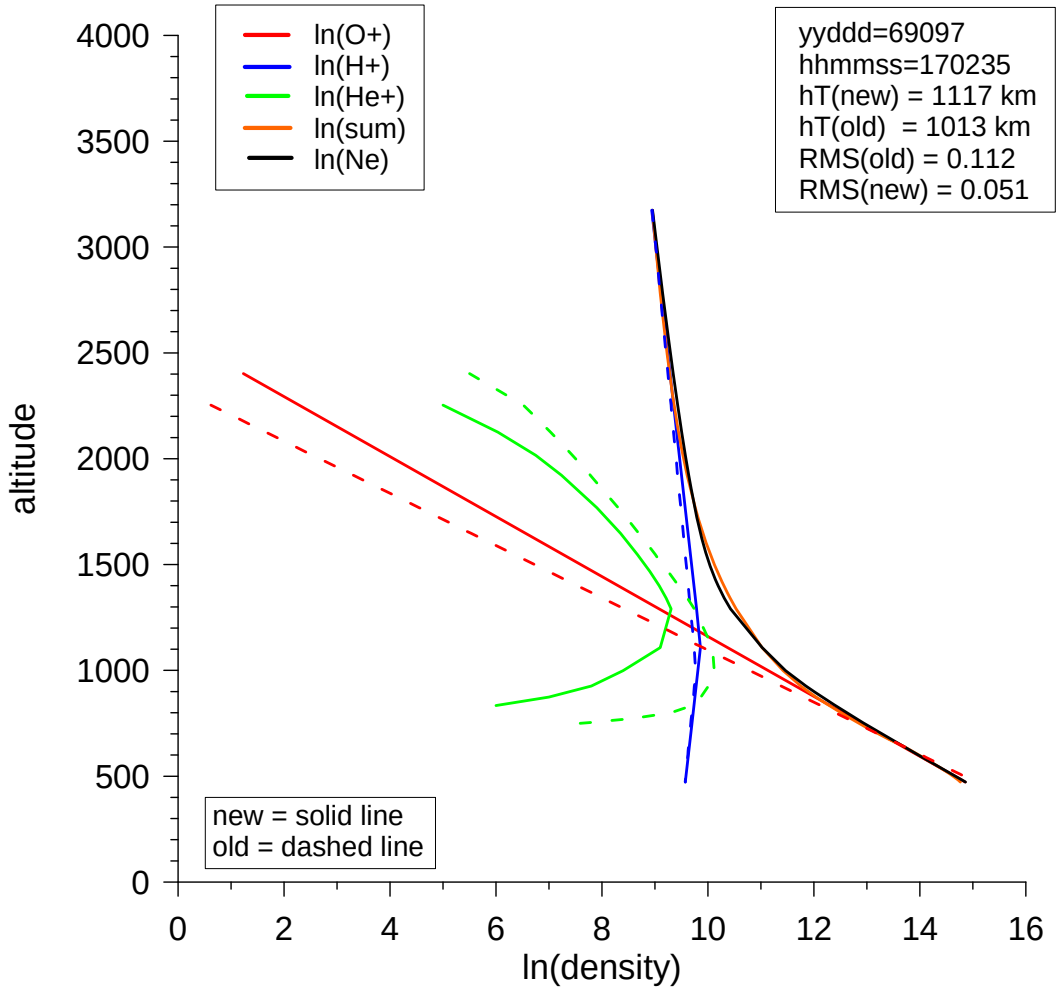

Figure 2: A sample profile measured on day 97 of year 1969, 17:03 UT around equator (lat = 12˚S, long=12.5˚E). Logarithm of ion density profiles obtained without optimization (denoted as "old") and those with optimization (denoted by "new"), are color coded, along with the measured Ne profile presented with the black line. The "old" profiles are presented by dashed lines, while the "new" profiles are given by solid lines. The total ion density presented the sum of the "new" profiles is given by the orange line.

The histogram of distribution of RMS errors collected from the whole selected ISIS-1 database containing 14,775 profiles is given in **Figure 3.** The pink filled bars represent histogram of RMS without optimization, while transparent blue bars show distribution of RMS error after optimization. The average RMS error without optimization is 0.189, while the average RMS error with optimization is 0.085. **Optimization reduced in average the model error 2.25 times.**

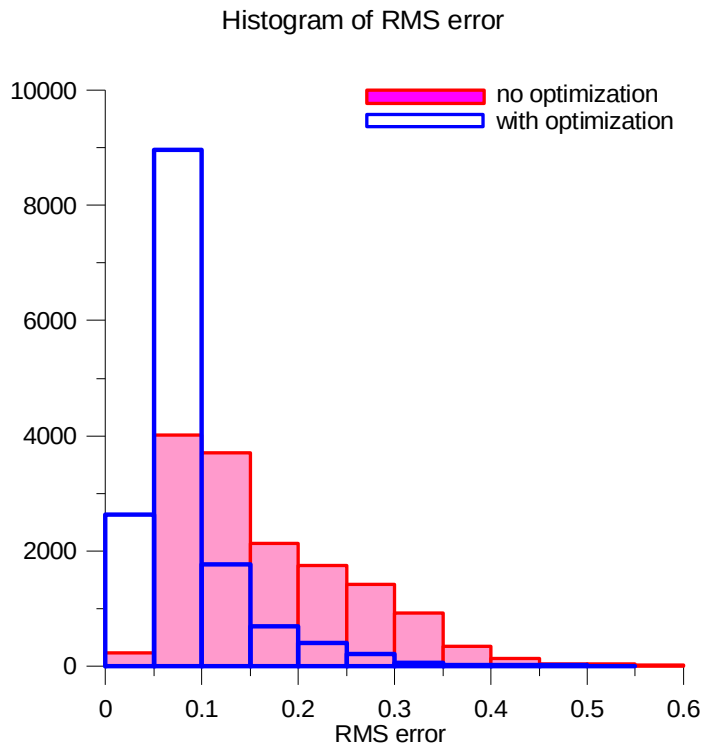

Figure 3: A histogram of distribution of RMS errors collected from the whole selected ISIS-1 database containing 14,775 profiles. The pink filled bars represent histogram of RMS without optimization, while transparent blue bars show distribution of RMS error after optimization.

1.2.2 Improvements of the TSMP formulation

The *g* function determines the presence of He^+ at transition height h_T and it is a key parameter for the reconstruction of the electron density. TaD cannot obtain any information about the He^+ from the bottomside sounding and therefore the presence of helium ions is *a priori* determined on the base of topside sounder profiles. For obtaining analytical expression for *g*, we reduced the ISIS-1 database, excluding profiles with g = 1. The latter restriction is necessary in order to exclude contribution of the profiles with no presence of He^+. To approximate *g* obtained from individual measured profiles (g = n(H+)/ n(O+)), we chose analytical function of three variables: local time, geomagnetic latitude and O^+ density. The latter variable was added to the first two after specifying the strong correlation between g and $n(O^+)$. The inclusion of $n(O^+)$ in analytical expression significantly reduced the model error, e.g. standard deviation between model and measured values.

Mathematical formulation

Coefficient matrix *CFN* is a solution of the problem for LSQ-approximation of the given data points ($x(k)$; $f(k)$), $x(k)=(x_1(k), x_2(k), x_3(k),)$, i.e. *CFN* minimizes the functional:

$$\sum_{k=1}^{N}\left(f(k)-F\left(CFN\ ,\ x(k)\right)\right)^2 \tag{4}$$

where $F(CFN,x) = F(x)$ is an element of the LSQ-approximation.

We define the function $F(x_1,x_2,x_3)$ within the intervals $[a_i,b_i]$, $[c_i,d_i]$, i=1,…,3; base-functions and coefficients as follows:

$$F(x_1,x_2,x_3)=\sum_{j_1=1}^{n_1}B_{1j_1}(s_1)\sum_{j_2=1}^{n_2}B_{2j_2}(s_2)\sum_{j_3=1}^{n_3}B_{3j_3}(s_3)CFN(j_1,j_2,j_3) \tag{5}$$

where:

$(x_1,x_2,x_3)\in \mathrm{R}^3$, $(s_1,s_2,s_3)\in \mathrm{R}^3$ *for* i=1,2,3

$x_i\in[a_i,b_i]$, $s_i\in[c_i,d_i]$, $s_i=c_i+\dfrac{x_i-a_i}{b_i-a_i}(d_i-c_i)$,

$CFN(i_1,i_2,i_3)$ are elements of coefficient matrix with a size $n_1\times n_2\times n_3$;

Base-functions are $B_{i,j}(s_i)$, $j=1,2,...,n_i$.

For the base-function we use:

Algebraic functions: $1, s, s^2, ..., s^k, ...$;

Tchebishev's functions: $T_0(s)=1$, $T_1(s)=s$,…, $T_k(s)=2sT_{k-1}(s) - T_{k-2}(s)$, for k=2,3, …,
i.e. $T_k(s)=\cos(k \arccos(s))$;

Trigonometric functions: 1, sin(s), cos(s), …, sin(ks), cos(ks), …;

In our case the base-function and coefficient, defined above, are:

$n_1=7$; $[a_1,b_1]=[0,24]$; $[c_1,d_1]=[0,2\pi]$; $B_{1,1}(s)=1$, $B_{1,2}(s)=\sin(s)$, $B_{1,3}(s)=\cos(s)$;....$B_{1,7}(s)=\cos(3s)$

$n_2=7$; $[a_2,b_2]=[-90,90]$; $[c_2,d_2]=\left[-\frac{\pi}{2},\frac{\pi}{2}\right]$; $B_{2,1}(s)=1$, $B_{2,2}(s)=\sin(s)$, ..., $B_{2,7}(s)=\sin(6s)$.

$n_3=5$; $[a_3,b_3]=[4,12]$; $[c_3,d_3]=[-1,1]$; $B_{3,1}(s)=1$, $B_{3,2}(s)=s$, $B_{3,3}(s)=2s^2-1$; $B_{3,4}(s)=4s^3-3s$....;

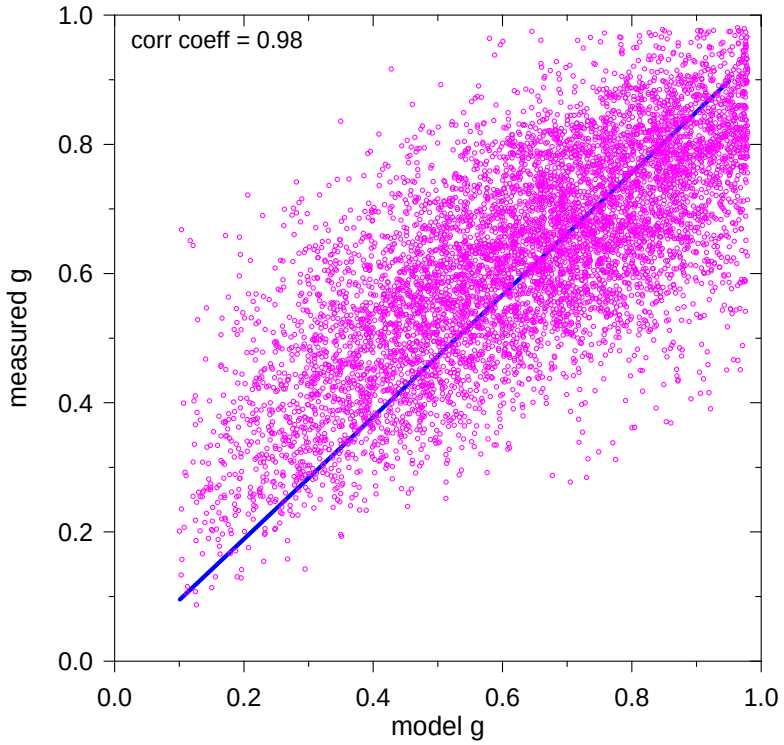

Figure 4: The scatter plot of model *g* (*gm*) versus measured *g* values. The thick blue line is the linear regression through the origin over *gm* values.

The scatter plot of model *g* (*gm*) versus measured *g* values is given in **Figure 4**. The thick blue line is the linear regression through the origin over *gm* values. Correlation coefficient is 0.98, which shows that the analytical function of g represents the data exceptionally well. Function *g* is a 3-D surface that could not be easily visualized. To get an idea how *g* function depends on each of the three variables, in **Figure 5** we have approximated the projection of *gm* values on each of axes plane with low order polynomials. In the top panel, the linear fit shows that *gm* have a tendency to decrease with increasing O^+ density. This means that He^+ predominantly appears (reversely proportional to *g*) when O^+ density increase, which happens at the F region anomaly crests. The middle panel shows that *gm* has a minimum of around 0.6 at low latitudes and increases toward higher latitudes, which complies with the known fact that He^+ is predominantly present around equator. Local time dependence shows a minimum in the early afternoon hours, when the equatorial anomaly is well developed. As a conclusion, we may say that *gm* behavior is in compliance with expected variation of He^+ density and the function can reliably estimate contribution of helium ions in transition region.

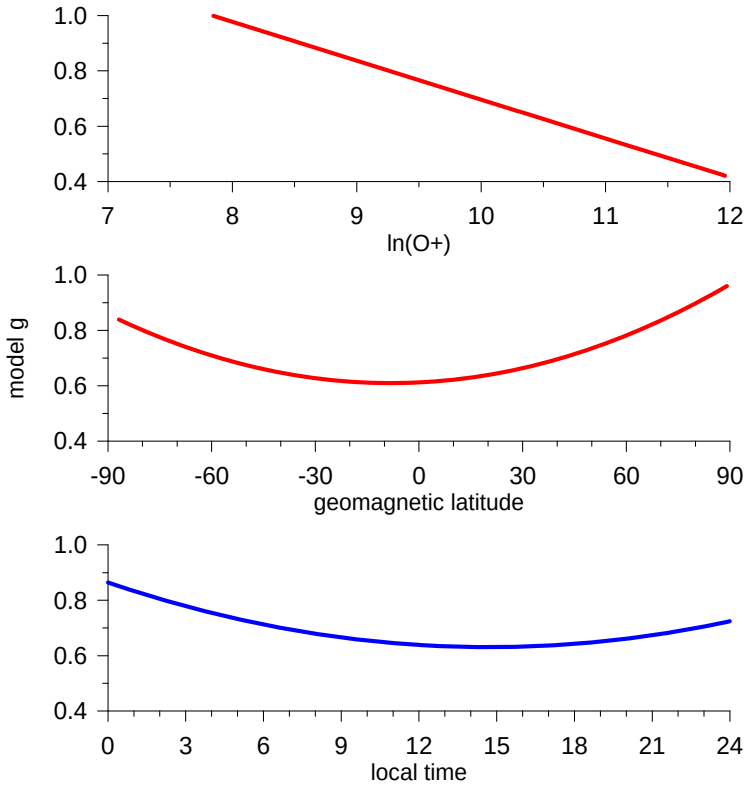

Figure 5: The projection of the function *gm* on each of axes plane with low order polynomials; Top panel: the linear fit shows that *gm* have a tendency to decrease with increasing O^+ density; Middle panel: *gm* has a minimum of around 0.6 at low latitudes and increases toward higher latitudes; Bottom panel: local time dependence shows a minimum in the early afternoon hours.

2. Validation of the new profiler

Validation is a strong requirement for implementation of a model for operational use. Model validation is the comprehensive, systematic quantitative comparison of model output with observations and is required for identifying and documenting model strengths and weaknesses. For the validation of the TaD profiler we have performed a systematic comparison of the model results with all available ground and space based observations. These datasets were identified through the state-of-art survey carried out within the framework of this project (Belehaki et al., 2009b) and include TEC data from ground-based GNSS receivers, partial TEC data from CHAMP mission and ISR EDP.

2.1 Comparison with measured profiles from ISIS-1

As a first test of the performance of the new profiler, we compared TaD electron density profiles with actual measurements obtained from ISIS-1 satellite. This is not an independent evaluation test as ISIS-1 profiles were used for the development of the new method, but provides with evidence of how well the new profiler reproduces the input measurements. The comparisons are made through the estimation of the RMSE over whole profile, according to the following formula:

$$RMSE = \frac{1}{np}\left\{\sum_{h_{\max}}^{h_{\min}}\left[n_{TaD}(h) - n_{ISIS1}(h)\right]^2\right\}^{1/2} \qquad (5)$$

where np indicates the number of points in each ISIS1 EDP, h_{min} and h_{max} are the lowest and highest altitudes for which ISIS1 electron density measurements are provided for a given profile, n_{TAD} and n_{ISIS1} are the electron density values at a given height h, provided by the TAD model and ISIS1 satellite respectively.

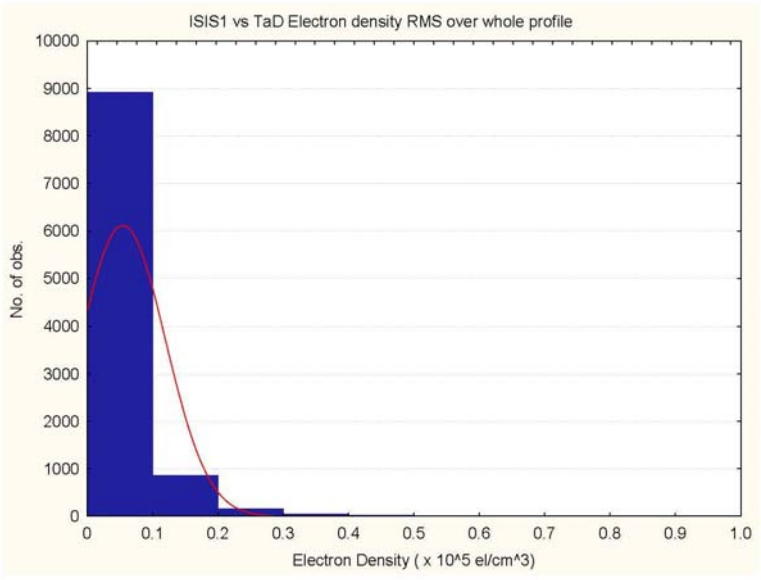

Figure 6: The histogram of distribution of RMSE between ISIS1 measured electron density and TaD output values.

The histogram of distribution of RMSE is presented in **Figure 6**, indicating a very successful fit between measurements and model predictions. This very good agreement can also be seen between the TEC parameters estimated by the ISIS1 profiles and those provided by the TaD model. In **Figure 7a** we present the correlation between the TEC parameter estimated for the plasmasphere region, integrating the electron density from the transition height up to the maximum height of the ISIS1 satellite. A very high correlation coefficient of 98.2% is estimated between the measured and the modeled parameters. Similarly, in **Figure 7b** we present the TEC parameter for the topside ionosphere, integrating from the lower height of the ISIS1 satellite (slightly above hmF2) up to the transition height. Here the correlation coefficient, between observed and modeled quantities, is also impressively high reaching the 99%.

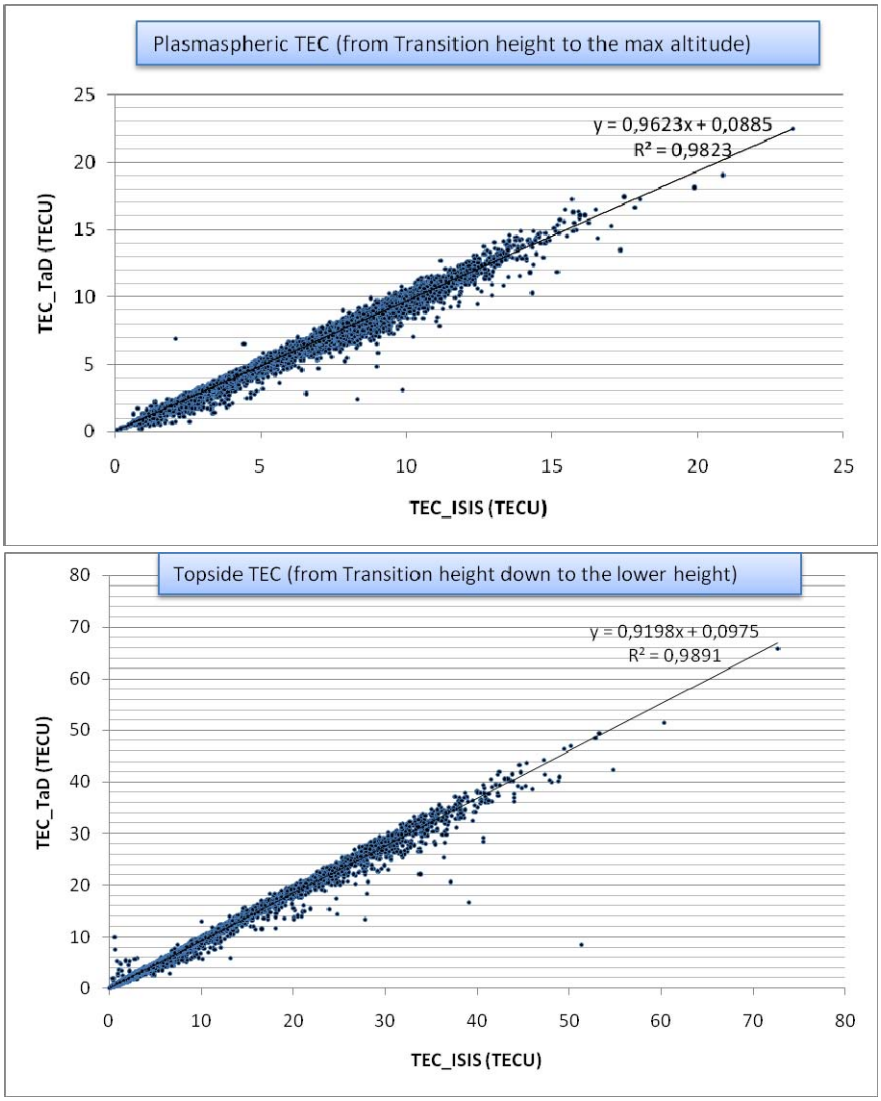

Figure 7: Scatter plots between the ISIS1 TEC parameter and the TaD TEC for (a) the plasmasphere region, integrating the electron density from the transition height up to the maximum height of the ISIS1 satellite and (b) the topside ionosphere, integrating from the lower height of the ISIS satellite (slightly above hmF2) up to the transition height.

2.2 Comparison with TEC derived from ground-based GNSS receivers

In this section, the comparison is based on TEC parameters estimated from data broadcasted by GNSS receiving stations and correspond to Athens (38.000N, 23.500E) and Juliusruh (54.600N, 13.40E) coordinates. The method of comparison is the following: the bottomside integral of Ne profile obtained from Digisonde ionograms is added to the integral of topside Ne profile obtained by TaD method and the sum is compared with TEC values obtained by GPS signals at the same locations. The database is compiled from ionosonde and corresponding GPS-TEC data at 30 min sampling compassing 5 years (2001-2005) period. To give the degree of agreement between the two products, the GPS-derived TEC and the TaD-derived TEC, we present their scatter plot for Athens and Juliusruh sites, in **Figures 8 and 9** respectively. With green we mark the regression line.

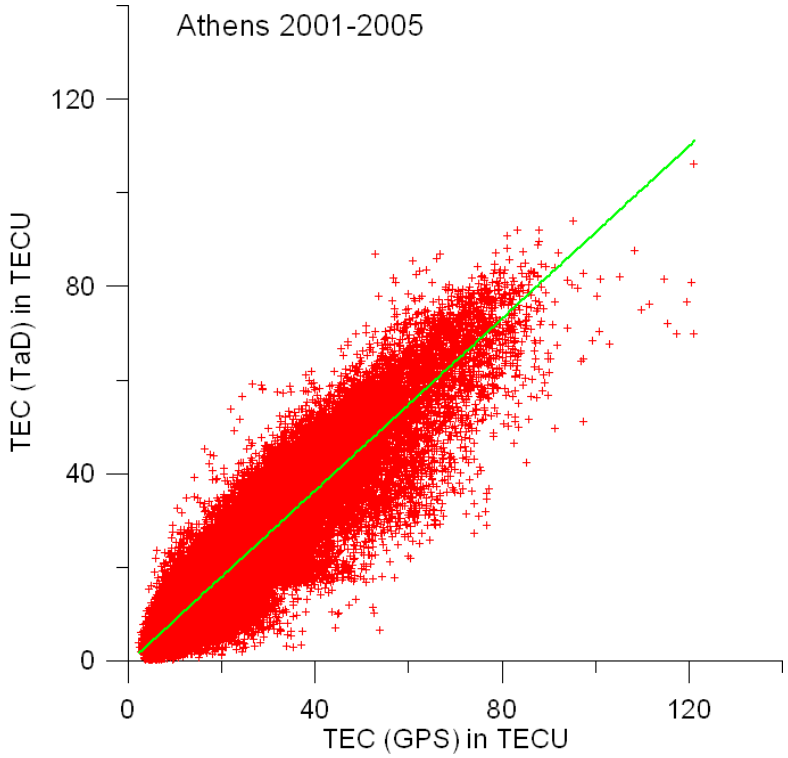

Figure 8: Comparison between GPS-derived TEC and TaD-derived TEC over Athens. Regression line is also plotted in green.

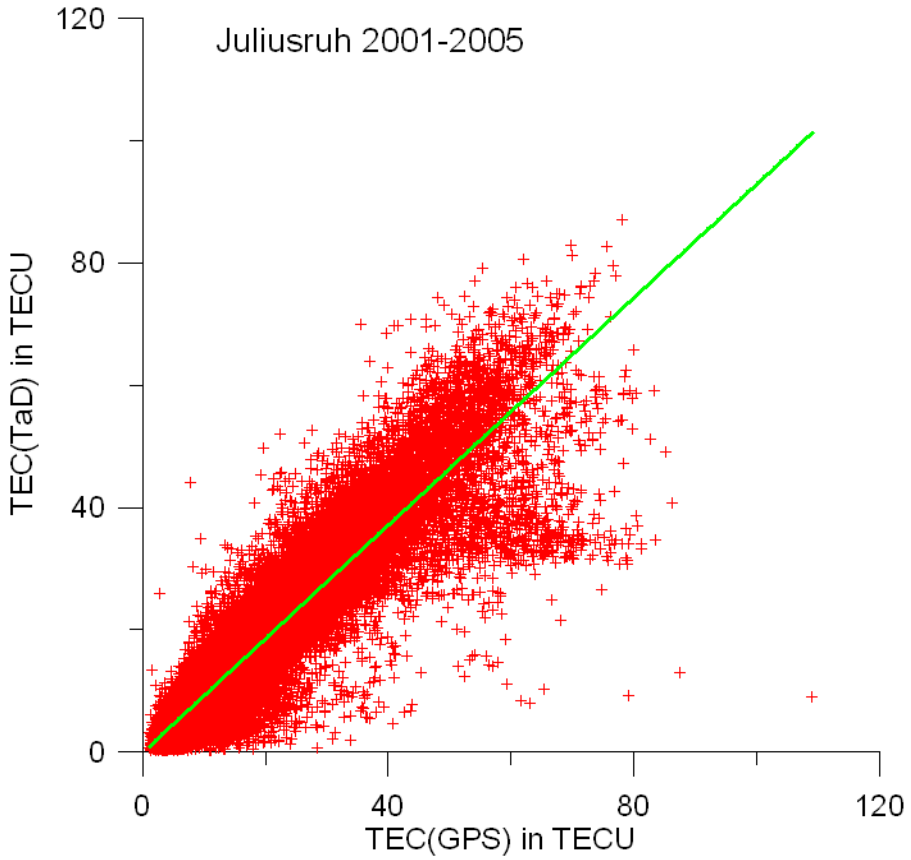

Figure 9: Comparison between GPS-derived TEC and TaD-derived TEC over Juliusruh. Regression line is also plotted in green.

It is important here to give a measure of the improvement of the TaD after its optimization. Table 1 gives the average value of the difference dTEC:

$$dTEC = TEC(TaD) - TEC(GPS)$$

on the whole sample of TEC parameters for each location, with the standard deviation of the population.

Table1: Improvement of the optimized TaD performance in respect to the original version, estimated for Athens and Juliusruh sites for the period 2001-2005

	Athens		**Juliusruh**	
	Original TaD	**Optimized TaD**	**Original TaD**	**Optimized TaD**
No of points	63,317		71,088	
dTEC mean value (TECU)	-1.9	-1.5	-1.0	-0.8
dTEC Standard Deviation (TECU)	5.3	3.4	2.9	1.9

2.3 Comparison with data from Malvern ISR

An important part of the improved TaD validation plan is the comparison of the model profiles with measured profiles obtained from Malvern ISR. This test provides information for the model's performance in the altitude zone 200-600 km (approximately). The importance of this test is threefold: i) ISR profiles are the only source of full electron density observation from the ground, ii) they consist a totally independent source of information and iii) this comparison is strongly suggested by US National Space Weather Program and recent studies for the establishment of the top high priority metric for the ionosphere-thermosphere domain. For this purpose, a data set of some of 4000 electron density profiles obtained at Malvern ISR site (52.1 ˚N, 2.3 ˚E) during the time interval 1968-1971 were analyzed. After quality check almost the 30% of profiles have been eliminated from our sample. The F layer peak density NmF2 and height hmF2 were extracted from each individual profile. However, for the scaling of the ISR EDPs we have applied the method used in the topside sounder profiles scaling, i.e. the NmF2 and hmF2 parameters have been located in each measured profile; then its topside scale height H_{TM} has been obtained as a regression line from a number of data points above the peak, with the transition height h_{TM} being approximated as the height where O^+ is one half of the measured density. The four quantities taken from the measured profile have been ingested to the formula (3) and the model profile was calculated for altitude range of the topside part of measured profile. Keeping this in mind, the analysis attempted below may be considered as a rough evaluation of the method's performance but in our opinion it provides suggestive conclusions.
Figure 10 gives some examples of the derived profiles.

Malvern-ISR profiles cover the altitude range up to approx. 700 km which is about the altitude of the actual transition height, so it is expected that O^+ will dominates and the observed Ne profile will follow closely the TaD profile of the O^+ density. Based on this, we first compared the model predictions for O+ distribution in respect to the measured profiles. The results are expressed in terms of the normalized RMSE estimates that where obtained over the topside profiles (from hmF2 up to the maximum height of the observed profiles). Their distribution is presented in **Figure 11.**
We also compared the observed Ne profiles with models predictions for the total density. The corresponding results for the normalized RMSE are presented in **Figure 12**.

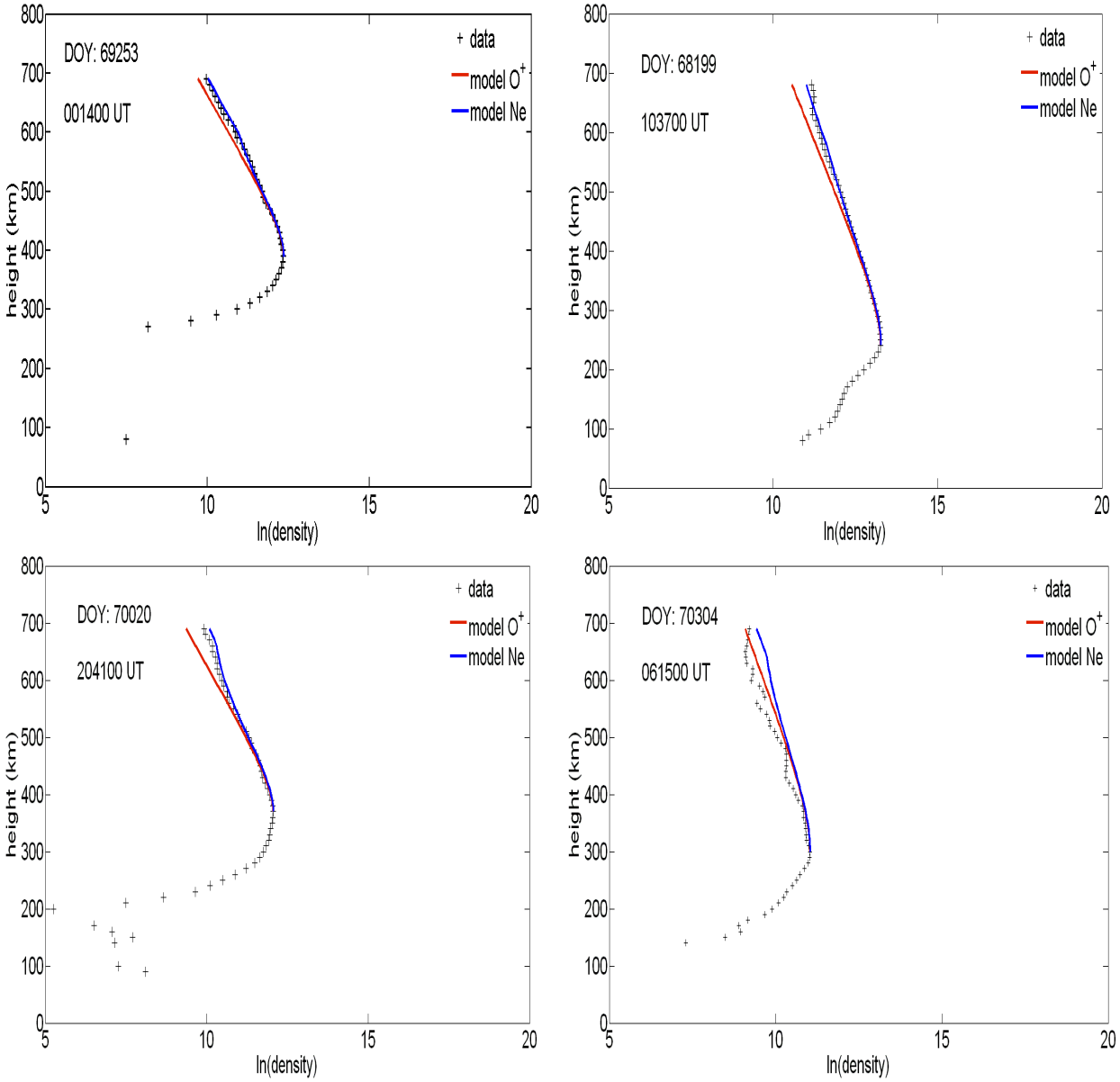

Figure 10: Examples for TaD derived profiles based at Malvern site. The ISR EDP are denoted with the cross symbol. Red line indicates the modeled O+ profile and blue line indicates the modeled EDP.

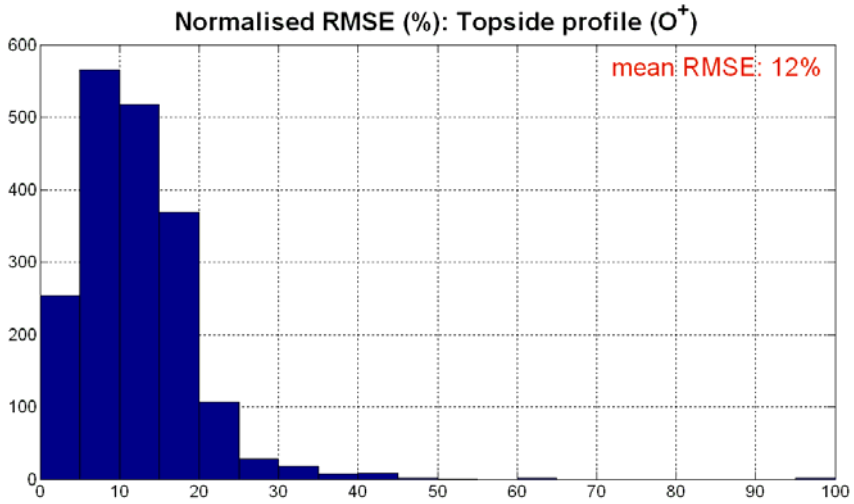

Figure 11: The normalized RMSE distribution of model predictions for O^+ in respect to the measured profiles.

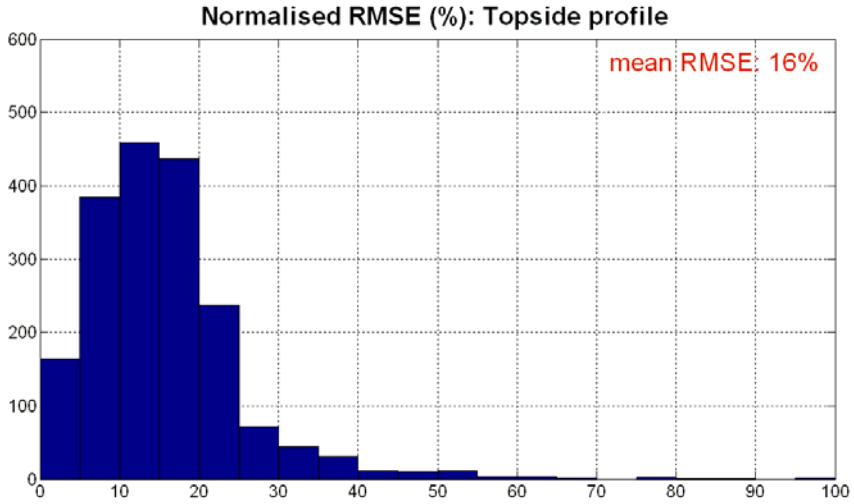

Figure 12: The normalized RMSE distribution of modeled total electron density in respect to the measured profiles.

The comparison between Figure 11 and 12 confirms our assumption for better fitting of the TaD O^+ profiles with the measured EDP.

Due to the fact that the topside ISR profiles are limited to 700 km, transition height cannot be always reliably obtained, e.g. we cannot reach the height where O^+ is one half of the measured density. Moreover, the measured profiles around their upper values exhibit an artificial increase which TaD wrongly is interpreted as appearance of H^+.

This might be the reason of the tendency of the model to overestimate the electron density, as seen in **Figure 13**. Here we present the distribution of the simple difference between the observed and the modeled electron densities at three selected altitudes: 400 km (top), 500 km (middle) and 600 km (bottom). Another interesting result concerning the dependence of the model's performance with the height is that the fit of the model to the observed values increases with increased altitude.

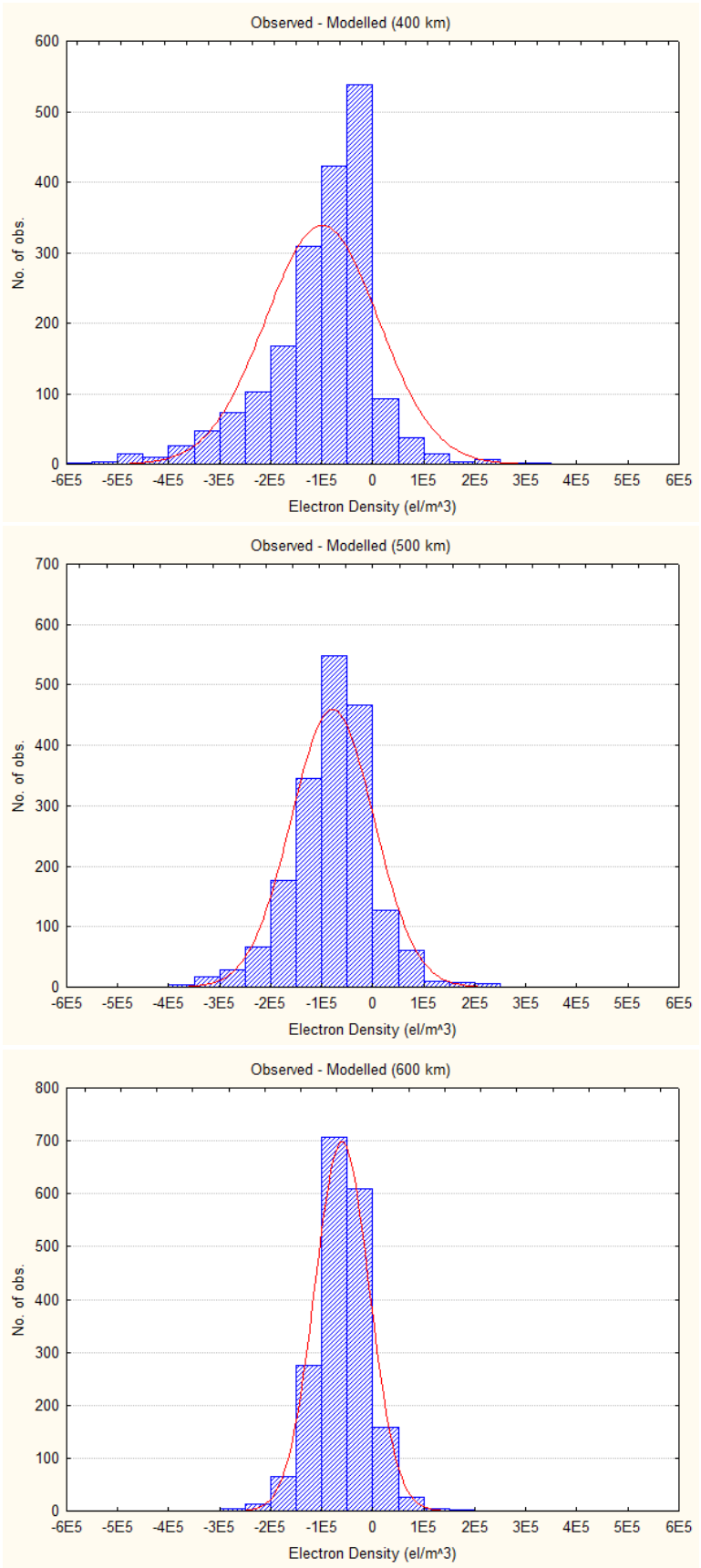

Figure 13: The distribution of the simple difference between the observed ISR and the modeled electron densities at 400 km (top), 500 km (middle) and 600 km (bottom).

As TEC is the most critical parameter for the reliable performance of several applications, we also performed comparison tests between TEC estimates obtained from modeled and observed EDP from the ISR at Malvern site concentrating in the topside part of the profile.
First, we present in **Figure 14** the scatter plot of TEC modeled versus TEC observed estimates. The results indicate that the two parameters correlate reasonably well. A larger scatter is seen in the daytime hours (the area with larger TEC values), which is probably due to the high altitude of the transition height, something that makes its accurate determination problematic due to the lack of observations above 700 km. The O^+ /H^+ transition height varies but seldom drops below 500 km at night or 800 km in the daytime, although it may lie as high as 1100 km, depending on the geophysical conditions, and particularly on solar activity (Denton et al., 1999).

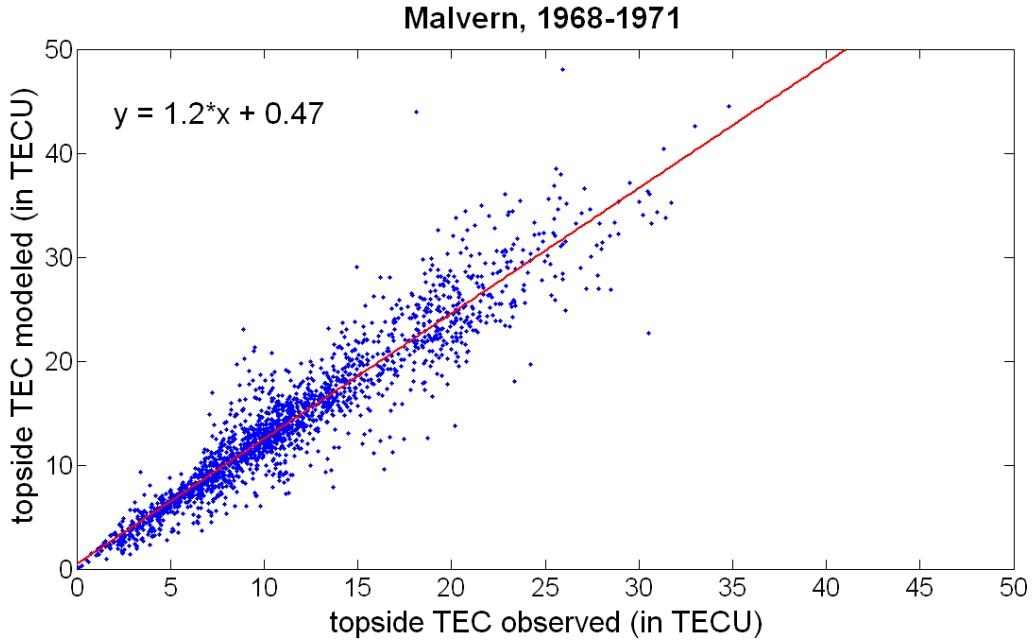

Figure 14: The scatter plot of TEC modeled versus TEC observed estimates

In **Figure 15** we present the TEC error (abs(TECobs-TECmod)) distribution and the relative TEC error distribution. From the top to the bottom we present the results based on all available measurement, in the middle we present the corresponding distribution diagrams for a subset of measurements that correspond to daytime EDP and in the bottom we give the distribution diagrams for nighttime cases. The analysis on the whole sample of measurements gives s mean error of 3TECU and mean relative error of 28.5%. However this error reduces considerably when we include only the nighttime cases. This is an additional evidence showing that during daytime, when the transition height is in its upper limits, or even higher of 700 km, there are not enough data for the TaD to estimate correctly the transition height and this yields to artificial results. The same problem was reported by Belehaki and Kersley (2006), where they compared the ISR EDP from Malvern with the results from the topisde extrapolation based on the Reinisch and Huang model (2001).

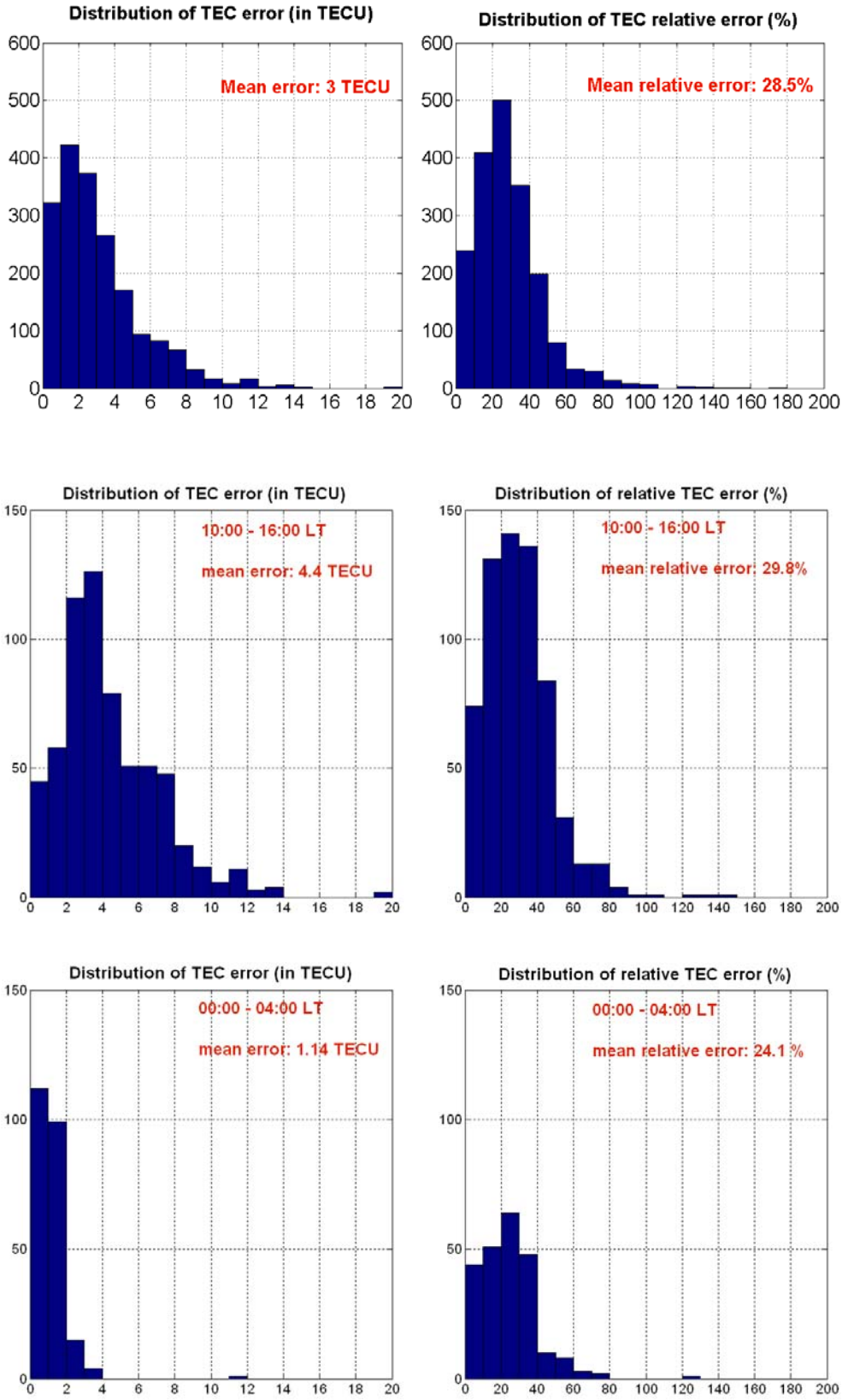

Figure 15: The TEC error (abs(TECobs-TECmod)) distribution and the relative TEC error distribution. From the top to the bottom: a) results based on all available measurements; b) the corresponding distribution diagrams for a subset of measurements that correspond to daytime EDP; c) the distribution diagrams for nighttime cases.

2.4 Summary on validation results

- The TaD model reproduces with very high accuracy the ISIS1 profiles demonstrating that the model does what it is designed to do and that it is free of intrinsic uncertainties.
- The model error of 3TECU is close to the measurement (GNSS) error
- The mean RMSE obtained from the comparison of ISR EDPs is in general larger than the RMSE obtained from the comparison with ISIS-1 profiles but this was expected as ISIS-1 profiles were also used for the model's development. The comparison with ISR EDPs gives a model's error mainly attributed to limitations imposed by the measured profiles themselves. During nighttime hours, when the transition height is lower than 700 km and can be determined by the TaD algorithm, the model values are in very high correlation with the ISR observations, with a mean error of only 1.14 TECU.

3. Definition of value-added products based on TaD model

The specification of value-added products is based on TaD functional capabilities, on the survey of related products available by various organizations worldwide and on latest needs specified by various users groups, identified in the frames of the European COST Action ES0803 “Developing Space Weather Products and Services in Europe”.
The functional capabilities of the TaD include: a) real-time calculation of the electron density up to GEO heights, at locations where a digisonde operate b) real-time calculation of TEC, and of its ionospheric and plasmaspheric portions c) real-time calculation of slab thickness and of its ionospheric part d) real-time availability of the partial TEC, whose altitude ranges may be defined by the user.
In addition the survey of related products indicated that worldwide there are several organizations providing TEC related products, however, we could not locate any web site of open access providing data of partial TEC. More precisely, the Space Weather Application Center in DLR, Germany, receives GPS data and calculates the following European products: TEC Map, Error Map, Rate of Change, Longitudinal Gradient, Latitudinal Gradient. The SPECTRE service in France, based on the same GPS data provides TEC maps, relative error maps and electronic biases. They also provide related STEC and VTEC products. In Japan, three research centers (Kyoto University, Nagoya University and the National Institute of Information and Communications Technology) provide TEC maps over Japan, over North America and over Europe based on GPS data. Global maps of TEC are provided by the MIT/Haystack Observatory in USA and by NASA in the standard IONEX format.
Latest needs specified by various users groups indicated that for a number of space activities we must partition GNSS TEC above and below the spacecraft in order to derive the TEC applicable to a particular activity. Such activities are the radar tracking of spacecraft as part of space surveillance programmes; the use of space-based synthetic aperture radars (SAR) to carry out remote sensing of the Earth’s surface; the use of on-board GNSS for small satellite missions.
Based on the above analysis it is evident that a model such as TaD able to provide the analytical function of the electron density up to GEO height would support a number of operational applications. As the operation of this model relies on the availability of ionospheric characteristics of the F-region, in Europe the TaD model could be integrated to the DIAS system (the European Digital Upper Atmosphere Server, http://dias.space.noa.gr) in order to make available a comprehensive set of services characterizing conditions in the topside ionosphere and the plasmasphere. However that set up of such a comprehensive service requires several steps including a) application of the TaD to as many as possible Digisonde locations b) development of mapping techniques over an area (such as Europe) c) computation of the 3D grid of ED values over the specified area.

Within the limited time of this project, we have been able to demonstrate the operation of TaD using as test site Athens, where a Digisonde operate and provides in real-time autoscaled ionospheric characteristics.

The flow chart of the set of web services providing the TaD output and the related value added products is shown in **Figure 16**.

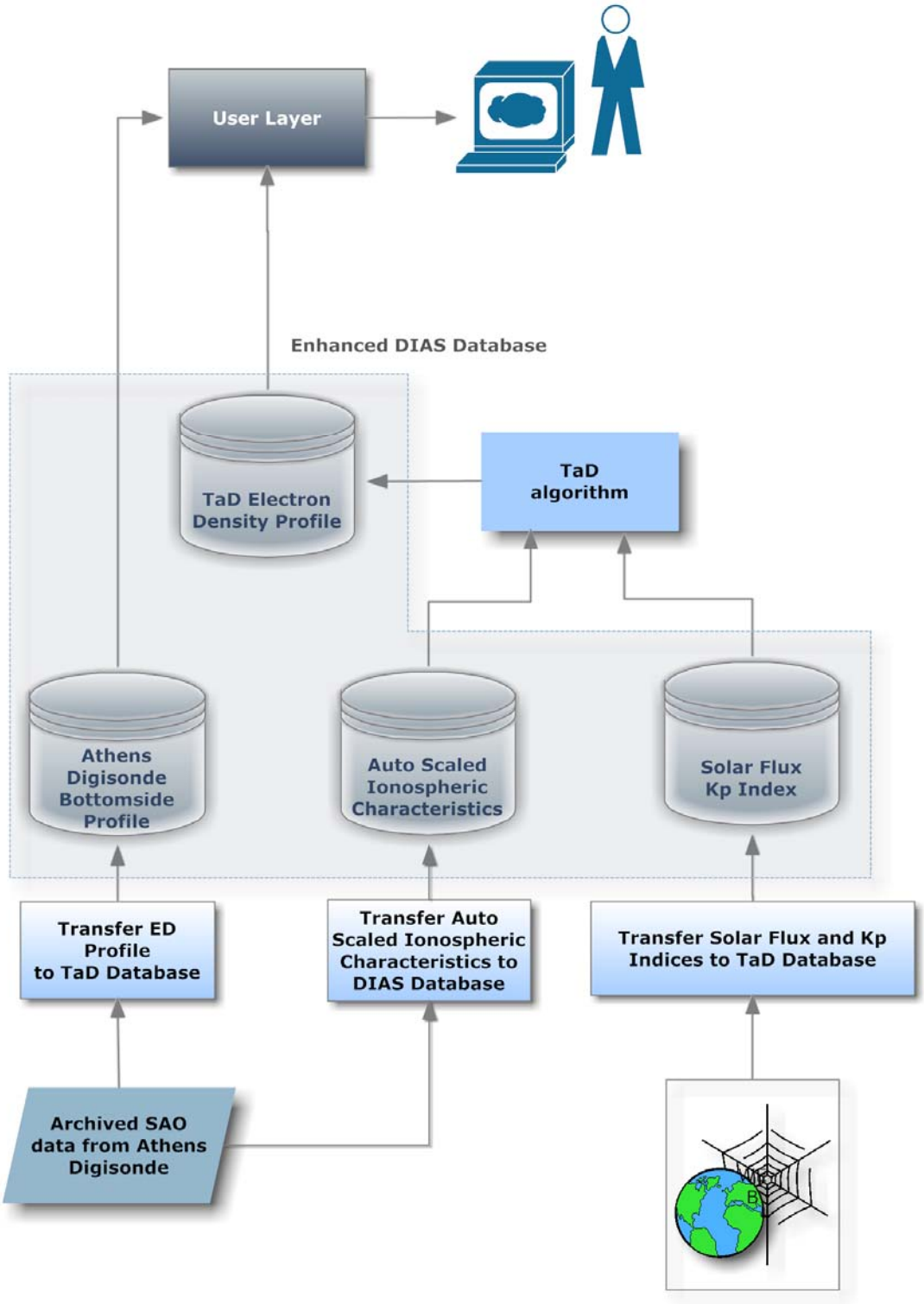

Figure 16: Flow chart of TaD web services

All TaD data and products are calculated with 15 min resolution. **The list of all available TaD related web services** is given below:

- The analytical function of the electron density profile up to 20,000 km in ASCII values
- Visualization of simultaneous ionograms and their corresponding TaD electron density extrapolated profile.
- The TEC up to 20,000 km, in daily plots
- The partial TEC corresponding to the plasmaspheric heights (from the transition height up to 20,000 km), in daily plots
- The partial TEC corresponding to the topside ionosphere (from the hmF2 up to transition height), in daily plots
- The slab thickness, in daily plots
- The ionospheric part of the slab thickness, in daily plots

4. On-line demonstration of the TaD results and value added products

A prototype service has been set up to demonstrate the functionality of the TaD algorithm and to distribute some indicative value-added products.
The service is available through the address:

http://www.iono.noa.gr/ElectronDensity/EDProfile.php

The web service has been developed with the following open source tools:

a) PHP, for the web services set up,
b) Perl, for the on-line implementation of TaD the algorithm that has been converted from its original FORTAN version
c) MySQL for the database, which was based on the enhancement of the DIAS database.

Below we present some screen shots to demonstrate the functionality of the web service.

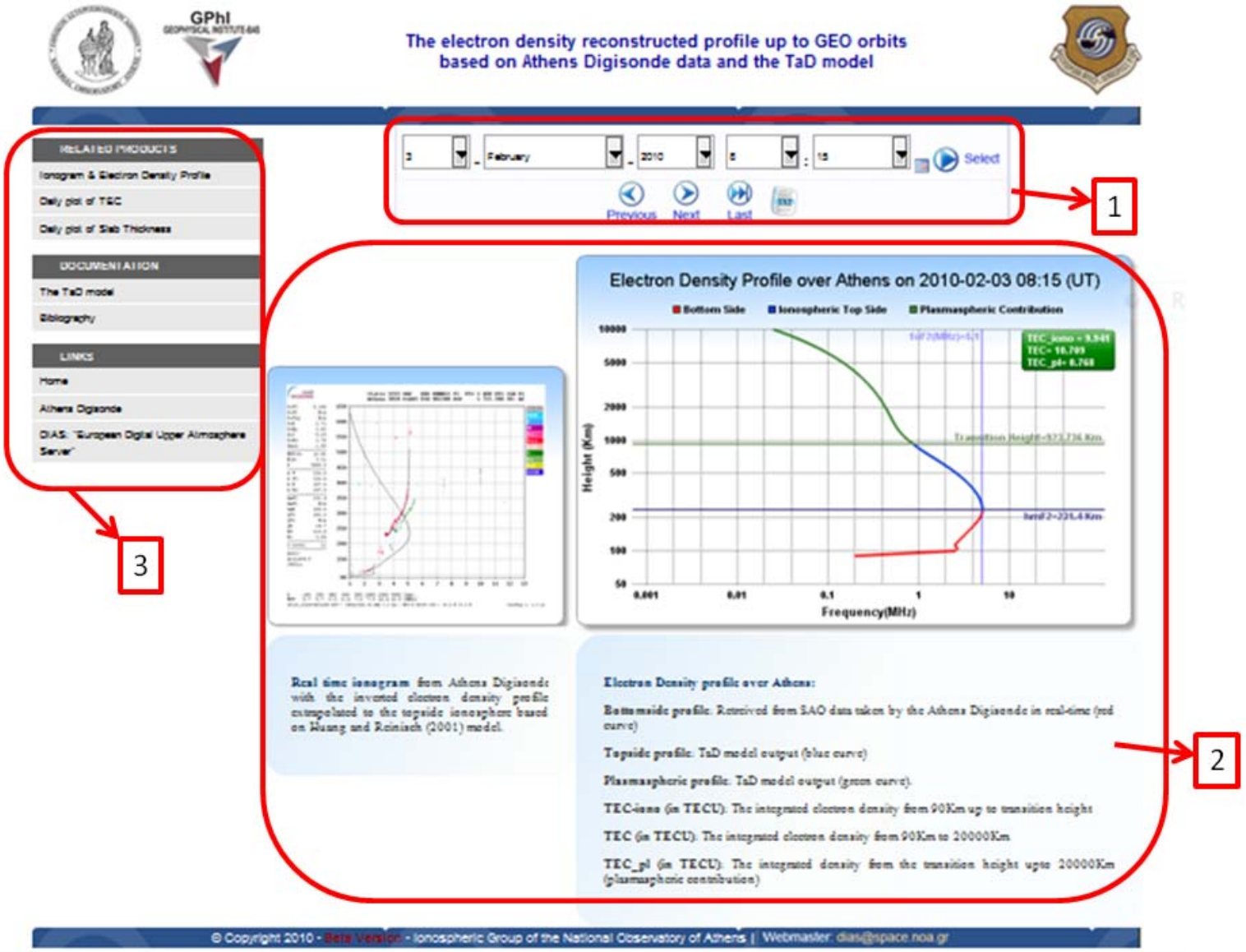

Figure 17: The Home Page of the TaD web services. Area (1) includes the main menu for quick search and for the download of the TaD EDP in ASCII. Area (2) includes the visualization of the TaD EDP and its corresponding ionograms. Area (3) includes the navigation buttons

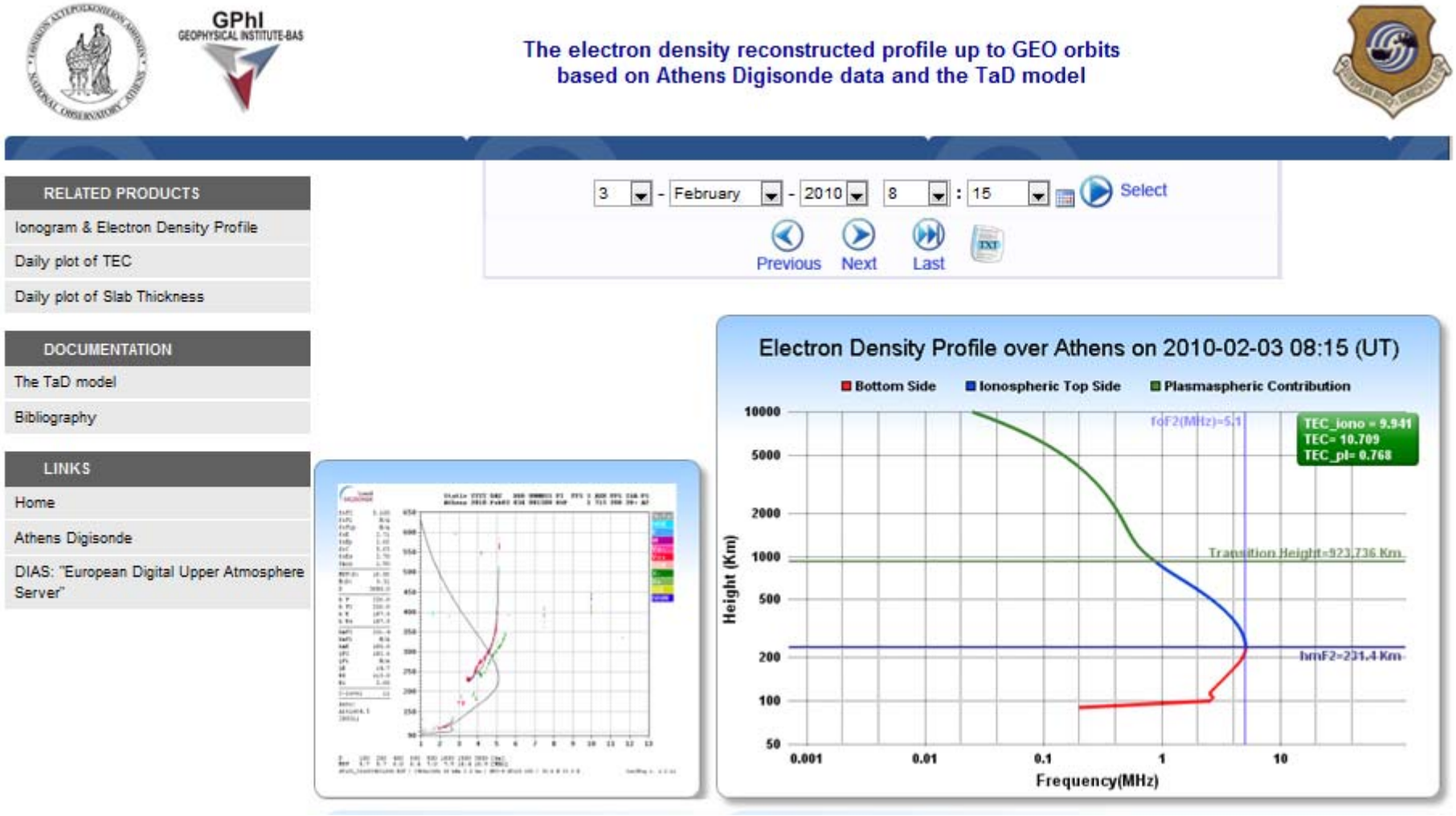

Figure 18: An enlarged view of the Home Page

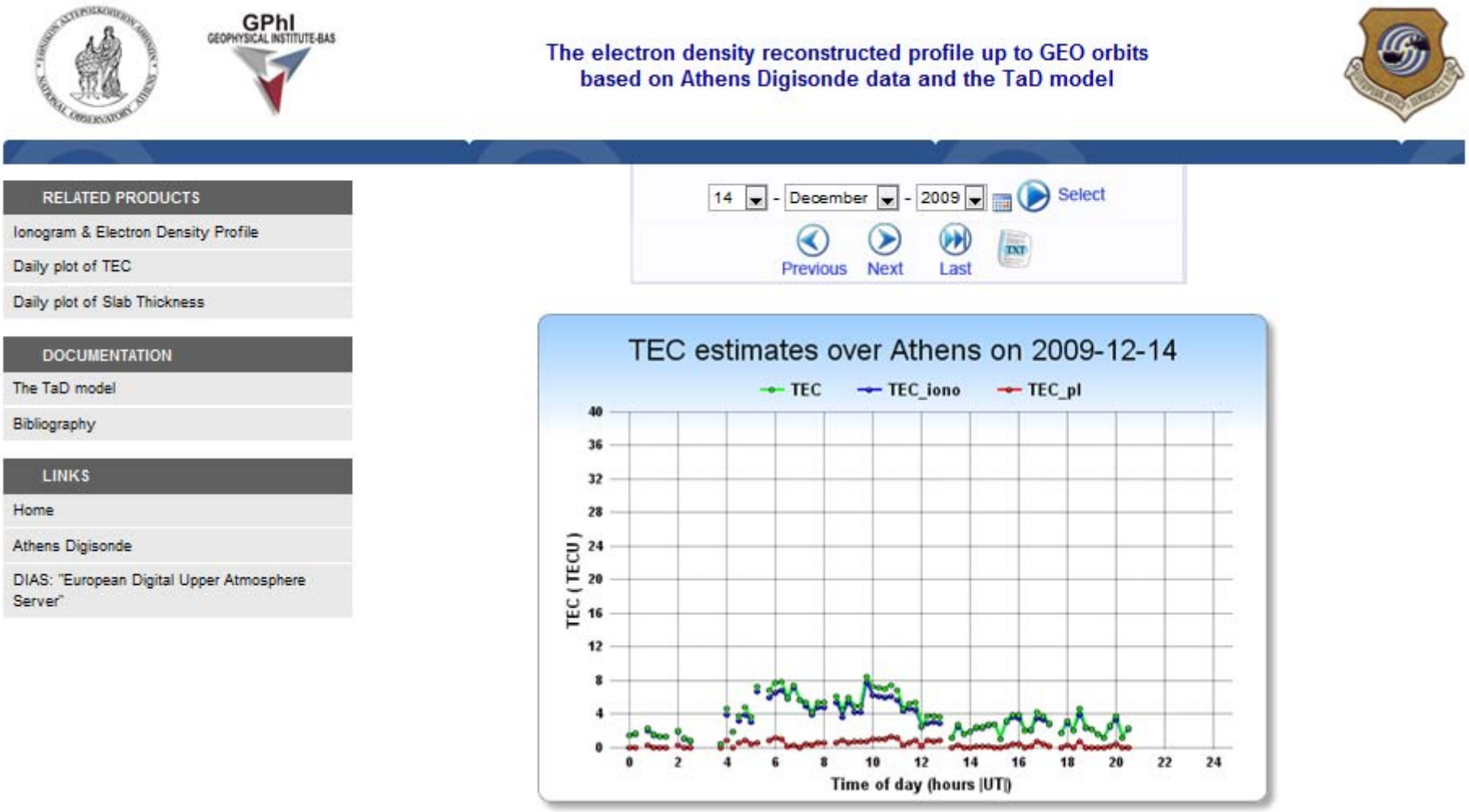

Figure 19: The daily plot of the various TEC parameters

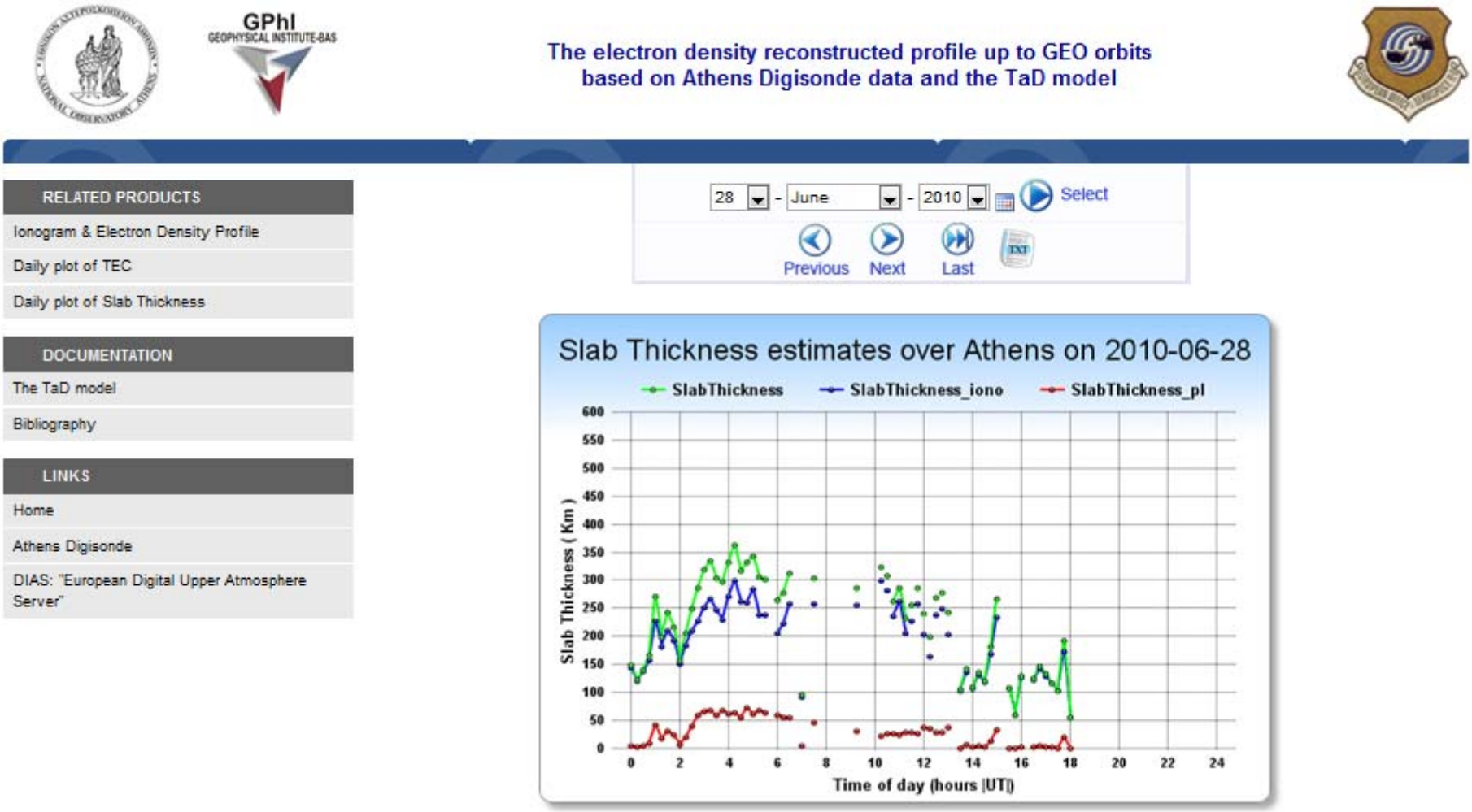

Figure 20: The daily plot of the slab thickness parameters

Electron Density Profile ascii data over Athens on 2010-02-03 08:15 (UT)
foF2(MHz)=5.1 hmF2(Km)=231.4 scale height F2(Km)=58.586
Transition Height(Km)=923.736 Kp=2.66667 Solar Flux=74

height(Km)	f(MHz) |TAD|	f(MHz) |Digisonde|
90.0		0.20000
100.0		2.54500
105.0		2.71000
110.0		2.58500
110.1		2.58200
115.1		2.58200
120.0		2.70500
120.2		2.71000
130.0		3.00000
140.0		3.27700
150.0		3.55300
160.0		3.83400
170.0		4.11600
180.0		4.38800
190.0		4.63000
200.0		4.82900
210.0		4.97400
220.0		5.06500
230.0		5.09900
231.4		5.10000
240.0	5.11533	
250.0	5.08638	
260.0	5.03950	
270.0	4.97747	
280.0	4.90283	
290.0	4.81789	
300.0	4.72465	
310.0	4.62491	
320.0	4.52021	
330.0	4.41189	
340.0	4.30111	
350.0	4.18884	
360.0	4.07589	
370.0	3.96298	
380.0	3.85067	
390.0	3.73943	
400.0	3.62966	
410.0	3.52167	
420.0	3.41571	
430.0	3.31198	
440.0	3.21063	
450.0	3.11177	
460.0	3.01549	
470.0	2.92183	
480.0	2.83084	
490.0	2.74253	
500.0	2.65688	
510.0	2.57390	
520.0	2.49355	
530.0	2.41581	
540.0	2.34062	
550.0	2.26796	
560.0	2.19777	
570.0	2.12999	
580.0	2.06459	
590.0	2.00150	
600.0	1.94067	

610.0	1.88204
620.0	1.82555
630.0	1.77116
640.0	1.71880
650.0	1.66843
660.0	1.61999
670.0	1.57342
680.0	1.52868
690.0	1.48571
700.0	1.44447
710.0	1.40490
720.0	1.36697
730.0	1.33062
740.0	1.29581
750.0	1.26249
760.0	1.23063
770.0	1.20018
780.0	1.17110
790.0	1.14334
800.0	1.11688
810.0	1.09167
820.0	1.06767
830.0	1.04485
840.0	1.02317
850.0	1.00259
860.0	0.98308
870.0	0.96460
880.0	0.94712
890.0	0.93060
900.0	0.91502
910.0	0.90033
920.0	0.88650
930.0	0.87148
940.0	0.85596
950.0	0.84110
960.0	0.82689
970.0	0.81329
980.0	0.80028
990.0	0.78783
1000.0	0.77592
1020.0	0.75362
1040.0	0.73320
1060.0	0.71449
1080.0	0.69734
1100.0	0.68160
1120.0	0.66714
1140.0	0.65384
1160.0	0.64157
1180.0	0.63025
1200.0	0.61976
1220.0	0.61003
1240.0	0.60098
1260.0	0.59253
1280.0	0.58463
1300.0	0.57721
1320.0	0.57023
1340.0	0.56364
1360.0	0.55739
1380.0	0.55145
1400.0	0.54579
1420.0	0.54038

1440.0	0.53518
1460.0	0.53019
1480.0	0.52538
1500.0	0.52072
1520.0	0.51621
1540.0	0.51183
1560.0	0.50757
1580.0	0.50341
1600.0	0.49935
1620.0	0.49538
1640.0	0.49149
1660.0	0.48767
1680.0	0.48392
1700.0	0.48023
1720.0	0.47659
1740.0	0.47301
1760.0	0.46948
1780.0	0.46600
1800.0	0.46256
1820.0	0.45916
1840.0	0.45580
1860.0	0.45247
1880.0	0.44918
1900.0	0.44592
1920.0	0.44270
1940.0	0.43950
1960.0	0.43633
1980.0	0.43320
2000.0	0.43009
2050.0	0.42242
2100.0	0.41492
2150.0	0.40756
2200.0	0.40034
2250.0	0.39326
2300.0	0.38630
2350.0	0.37948
2400.0	0.37277
2450.0	0.36619
2500.0	0.35973
2550.0	0.35338
2600.0	0.34714
2650.0	0.34101
2700.0	0.33500
2750.0	0.32908
2800.0	0.32328
2850.0	0.31757
2900.0	0.31197
2950.0	0.30646
3000.0	0.30106
3050.0	0.29575
3100.0	0.29053
3150.0	0.28540
3200.0	0.28037
3250.0	0.27542
3300.0	0.27056
3350.0	0.26579
3400.0	0.26110
3450.0	0.25649
3500.0	0.25196
3550.0	0.24752
3600.0	0.24315

3650.0	0.23886
3700.0	0.23465
3750.0	0.23051
3800.0	0.22644
3850.0	0.22245
3900.0	0.21852
3950.0	0.21467
4000.0	0.21088
4050.0	0.20716
4100.0	0.20350
4150.0	0.19991
4200.0	0.19638
4250.0	0.19292
4300.0	0.18951
4350.0	0.18617
4400.0	0.18289
4450.0	0.17966
4500.0	0.17649
4550.0	0.17338
4600.0	0.17032
4650.0	0.16731
4700.0	0.16436
4750.0	0.16146
4800.0	0.15861
4850.0	0.15581
4900.0	0.15306
4950.0	0.15036
5000.0	0.14771
5100.0	0.14254
5200.0	0.13756
5300.0	0.13275
5400.0	0.12810
5500.0	0.12362
5600.0	0.11930
5700.0	0.11513
5800.0	0.11110
5900.0	0.10722
6000.0	0.10347
6100.0	0.09985
6200.0	0.09635
6300.0	0.09298
6400.0	0.08973
6500.0	0.08659
6600.0	0.08356
6700.0	0.08064
6800.0	0.07782
6900.0	0.07510
7000.0	0.07247
7100.0	0.06994
7200.0	0.06749
7300.0	0.06513
7400.0	0.06285
7500.0	0.06065
7600.0	0.05853
7700.0	0.05649
7800.0	0.05451
7900.0	0.05260
8000.0	0.05076
8100.0	0.04899
8200.0	0.04727
8300.0	0.04562

8400.0	0.04403
8500.0	0.04249
8600.0	0.04100
8700.0	0.03957
8800.0	0.03818
8900.0	0.03685
9000.0	0.03556
9100.0	0.03431
9200.0	0.03311
9300.0	0.03196
9400.0	0.03084
9500.0	0.02976
9600.0	0.02872
9700.0	0.02771
9800.0	0.02674
9900.0	0.02581
10000.0	0.02491
10250.0	0.02279
10500.0	0.02085
10750.0	0.01907
11000.0	0.01745
11250.0	0.01596
11500.0	0.01460
11750.0	0.01336
12000.0	0.01222
12250.0	0.01118
12500.0	0.01023
12750.0	0.00936
13000.0	0.00856
13250.0	0.00783
13500.0	0.00716
13750.0	0.00655
14000.0	0.00600
14250.0	0.00549
14500.0	0.00502
14750.0	0.00459
15000.0	0.00420
15250.0	0.00384
15500.0	0.00351
15750.0	0.00322
16000.0	0.00294
16250.0	0.00269
16500.0	0.00246
16750.0	0.00225
17000.0	0.00206
17250.0	0.00189
17500.0	0.00172
17750.0	0.00158
18000.0	0.00144
18250.0	0.00132
18500.0	0.00121
18750.0	0.00111
19000.0	0.00101
19250.0	0.00092
19500.0	0.00085
19750.0	0.00077
20000.0	0.00071

Figure 21: The analytical function of the electron density profile up to 20,000 km in ASCII values downloadable from the main menu of the Home Page

5. Further steps

As a next step we propose the implementation of TaD in DIAS system (http://dias.space.noa.gr) to make available the TaD EDP at all DIAS locations (Athens, Rome, Ebro, Arenosillo, Pruhonice, Chilton, Juliusruh, Moscow) and consequently to be able to provide important services, such as, maps of TEC and of its time derivative, maps of plasmaspheric TEC, maps of slab thickness, 3D maps of electron density over Europe. This plan requires

a) application of the TaD to as many as possible DIAS locations and if possible to additional sites

b) development of mapping techniques over an area (such as Europe)

c) upgrade of the DIAS user layer profile

For the operational release of the system the following important issues must be considered related to the quality of real-time autoscaled ionospheric data:

- Automatic scaling errors affecting the TaD performance
- Data gaps
- Definition of the reference level in order to determine a disturbance index

The implementation of this plan is subject to the availability of the necessary funding resources.

References

Belehaki, A., P. Marinov, I. Kutiev, N. Jakowski, and S. Stankov, Comparison of the topside ionosphere scale height determined by topside sounders model and bottomside Digisonde profiles, Adv. Space Res, 37, 5, 963-966, 2006.

Belehaki A. and L. Kersley, Statistical validation of a technique for estimating total electron content from bottomside ionospheric profiles, *Radio Science*, 41, RS5003, doi: 10.1029/2005RS003433, 2006.

Belehaki, A., I. Kutiev, B. Reinisch, N. Jakowski, P. Marinov, I. Galkin, C. Mayer, I. Tsagouri, and T. Herekakis, Verification of the TSMP-assisted Digisonde (TaD) topside profiling technique, Acta Geophysica, 58, 3, 432-452, 2009a.

Belehaki A., I. Kutiev, I. Tsagouri, An improved model for operational specification of the electron density structure up to geosynchronous heights, AOARD FA5209-09-P-0253, Interim report, 2009b

Bilitza, D, International Reference Ionosphere (IRI)–Task Force Activity Report 2000, *IRI News*, **8**, 1/2, 8-15, June 2001.

Daniell, R.E., Jr., Brown, L.D., Anderson, D.N., Fox, M.W., Doherty, P.H., Decker D.T., Sojka J.J., and Schunk, R.W., Parameterized ionospheric model: A global ionospheric parameterization based on first principle models, Radio Sci., 30 (5), 1499-1510, 1995.

Heelis, R.A., W.B. Hanson, and G.J. Bailey, Distribution of He^+ at middle and equatorial latitudes during solar maximum, J. Geophys. Res., 95, 10,313-10,320, 1990.

Hochegger, G., Nava, B., Radicella, S.M., Leitinger, R. A family of ionospheric models for different uses, Phys. Chem. Earth 25 (4), 307–310, 2000

Kutiev, I., P. Marinov, S. Watanabe , Model of topside ionosphere scale height based on topside sounder data, Adv. Space Res., 37, 5, 943-950, 2006.

Kutiev, I. and P. Marinov, Topside sounder model of scale height and transition height characteristics of the ionosphere, Adv. Space Res., 39, 759-766, doi:10.1016/j.asr.2006.06.013, 2007

Kutiev I., P. Marinov, A. Belehaki, and B. Reinisch, N. Jakowski, Reconstruction of topside density profile by using the Topside Sounder Model Profiler and Digisonde data, Adv. Space Res., 43, 1683-1687, 2009a.

Kutiev I., P. Marinov, A. Belehaki, N. Jakowski, B. Reinisch, C. Mayer, and I. Tsagouri, Plasmaspheric electron density reconstruction based on the Topside Sounder Model Profiler, Acta Geophysica, 58, 3, 420-431, 2009b.

Kutiev, I., Belehaki, A., Marinov, P., Tsagouri, I., Fidanova, S., New Advances in Model Reconstruction of the Topside Electron Density Profiles, to be presented in the Sixth European Space Weather Week, 16-20 November 2009, Brugge, Belgium, 2009c

Moffett, R.J., and W.B. Hanson, Calculated distribution of hydrogen and helium ions in the low-latitude ionosphere, J. Atm. Terr. Phys., 35, 207-222, 1973.

Radicella, S.M., Leitinger, R. The evolution of the DGR approach to model electron density profiles. Adv. Space Res. 27 (1), 35–40, 2001.

Reinisch, B.W. and Huang, X., Deducing topside profiles and total electron content from bottomside ionograms, Adv. Space Res. 27, 1 pp. 23-30, 2001.

Stankov, S., N. Jakowski, S. Heise, P. Muhtarov, I. Kutiev, R. Warnant, A new method for reconstruction of the vertical electron density distribution in the upper ionosphere and plasmasphere , J. Geophys. Res., 108(**A5**), 1164, 2003. doi.10.1029/2002JA009570.

Stankov S.M., P. Marinov and I. Kutiev, Comparison of NeQuick, PIM, and TSM model results for the topside ionospheric plasma scale and transition heights, Adv. Space Res., 39, 767-773, 2007

Su, S.-Y., C.K. Chao, H.C. Yeh, and R.A. Heelis, Seasonal and latitudinal distribution of dominant light ions at 600 km topside ionosphere from 1999 to 2002, J. Geophys. Res., 110, 2005, A01302. doi:10.1029/2004JA010564